Nuclear Physics B204 (1982) 173–188

CORRELATIONS BETWEEN HIGH-MOMENTUM SECONDARIES IN pp COLLISIONS AT $\sqrt{s}$ = 44.7 AND 62.3 GeV

G.J. BOBBINK[1], M.A. VAN DRIEL, F.C. ERNÉ, W.G.J. LANGEVELD and J.C. SENS

National Institute for Nuclear and High Energy Physics, Amsterdam, The Netherlands

D. FAVART and P. LELEUX

Université Catholique de Louvain, B-1348 Louvain-la-Neuve, Belgium

M.M. BLOCK, R. CAMPANINI[2] and H.W. LUDWIG[3]

Northwestern University, Evanston, Illinois 60201, USA

M.A. BOTJE, R.J. GOOSSENS, B. VAN UITERT and D.A. VAN WEZEP

State University, Utrecht, The Netherlands

Received 29 March 1982

In pp collisions at $\sqrt{s}$ = 44.7 and 62.3 GeV, where each proton fragments into at least one low-p_T, high-x meson or baryon, no correlations between the particle momenta are found for $\pi\pi$, πK, KK, and pπ pairs. The $\pi\pi$ data show a preference for the formation of electrically neutral $\pi\pi$ systems. The KK data show the influence of strangeness conservation. For pp and pΛ final states, the momentum dependence of the correlation ratio R can be described by the scaling variable $z = (1 - x_1)(1 - x_2)$. Small deviations from factorization are discussed.

1. Introduction

The study of high-energy collisions in which one or two particles are produced with momenta near the boundaries of phase space (mostly high p_T and $x = 2p_L/\sqrt{s} \approx 0$ or low p_T and high x) is motivated by the fact that such reactions more readily exhibit the basic quark/gluon structure of the interacting particles than do most of the particle-production reactions. Experiments on the momentum distribution of low-p_T, high-x secondaries [1] and on the correlations between two low-p_T, high-x, back-to-back pions [2] are consistent with the view that such mesons are made up of

[1] Now at CERN, Geneva, Switzerland.
[2] Now at University of Bologna, Bologna, Italy.
[3] Now at ANL, Argonne, Illinois 60439, USA.

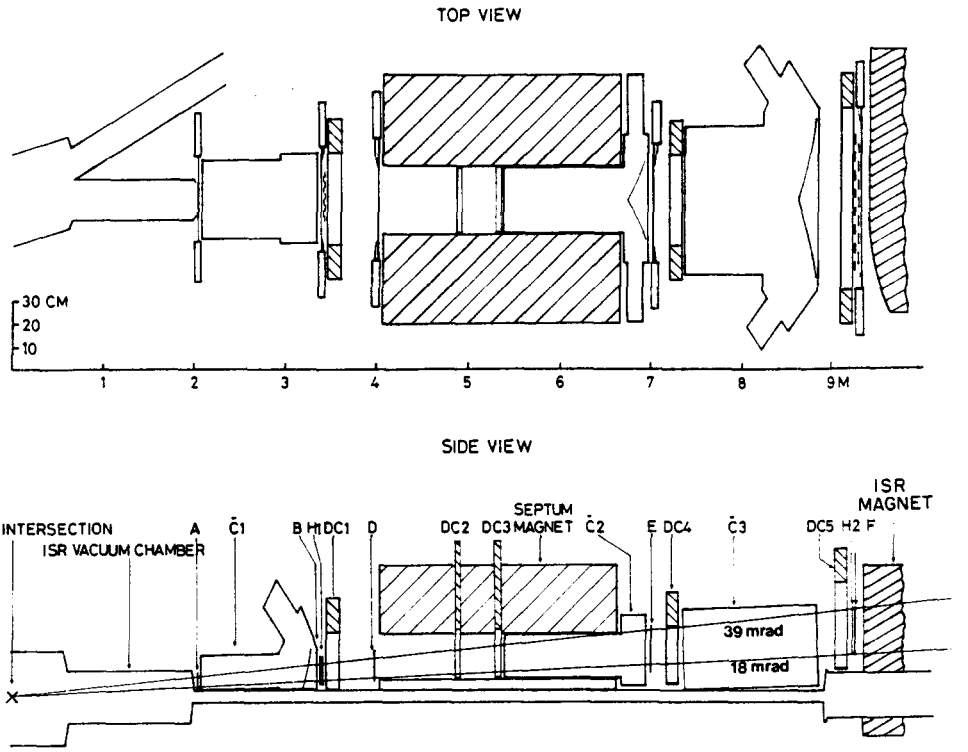

Fig. 1. Top and side view of one of the R607 spectrometers. The two spectrometers are identical and are mounted above the downstream ISR vacuum pipes.

the valence quarks of the proton in a process of gluon exchange. In the measurements to be discussed, our earlier correlation studies of $\pi\pi$ pairs at $\sqrt{s} = 62.3$ GeV [2] have been extended to include $\pi\pi$, πK, KK, pπ, pK, and pp pairs at $\sqrt{s} = 44.7$ GeV, and pΛ pairs at $\sqrt{s} = 44.7$ and 62.3 GeV. We observe that, as in the $\pi\pi$ case reported earlier, dynamic correlations, i.e. correlations between the momenta of the particles, are absent.

The data were taken with the R607 small-angle spectrometers at the CERN Intersecting Storage Rings (ISR). The spectrometers (see fig. 1) were located above the downstream vacuum pipes of one intersection of the CERN ISR and have been described in detail elsewhere [2, 3]. Each arm consists of a septum magnet, with $\int B\,\mathrm{d}l = 2.1$ Tm, trigger counters (A, B, D, E, F), 24 drift chamber planes arranged in 5 modules (DC1–DC5), 2 scintillation counter hodoscopes (H_1, H_2) and 3 atmospheric Čerenkov counters ($\check{C}_1, \check{C}_2, \check{C}_3$). The acceptance per arm is ~ 1 msr and covers vertical angles between 18 and 39 mrad with respect to the beam. The resolution (1 standard deviation) in momentum varied nearly linearly from 0.4% at 5 GeV to 1.0% at 31 GeV. Momenta smaller than 5 GeV were rejected at the trigger level.

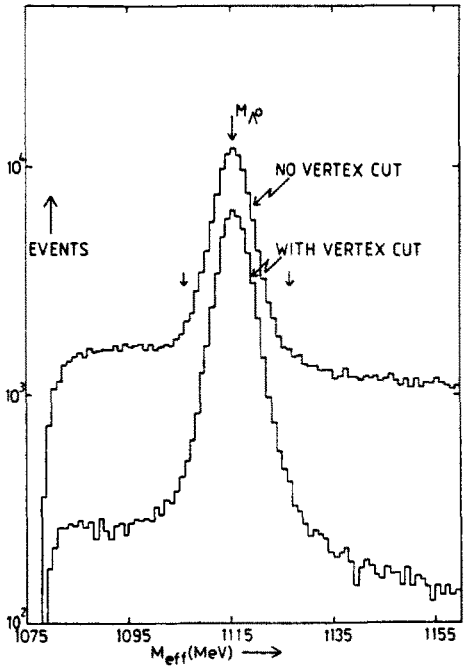

Fig. 2. Effective mass spectrum for neutral two-track events, assuming the positive particle to be a proton, the negative a π^-. Events "with vertex cut" originate at a distance of 0.5 to 1.8 m from the pp collision point. The arrows indicate the mass range identified as Λ's.

The overall trigger consisted of an Arm 1, an Arm 2, and an Arm 1 · Arm 2 trigger running in parallel. Each arm was triggered by a combination of scintillator, Čerenkov, and hodoscope matrix pattern requirements, set to select specific particle types and intervals in momenta.

At a luminosity $L = 2 \times 10^{31}$ cm^{-2} s^{-1}, the single-arm rate of the scintillator coincidences alone was ~ 30 kHz and consisted, for 98%, of beam-beam events. With the full trigger the single-arm rate was 6 kHz and the double-arm rate 30–50 Hz. Data were taken at $\sqrt{s} = 44.7$ (62.3) GeV for 1000 (2000) hours and with integrated luminosities of 2.8 (6.1) $\times 10^{37}$ cm^{-2}.

Momenta, angles, and particle types were determined following standard tracking and Čerenkov selection methods. In the sample of Λ triggers Λ's were identified as neutral two-track events peaking in the mass range $1106 < M < 1126$ MeV (see fig. 2). By applying vertex cuts the background under the peak could be reduced by a factor of 6 at the expense of a 50% reduction in signal. The mass resolution was approximately 3 MeV.

For each combination of particles the data were analysed in terms of two ratios, the correlation quotient Q and the correlation ratio R. The correlation quotient Q is

defined as

$$Q(x_1, x_2) = \frac{N_{12}(x_1, x_2)n}{n_1(x_1)n_2(x_2)}, \tag{1}$$

with $N_{12}(x_1, x_2)$ the number of collected events per unit x_1, x_2, $n_1(x_1) = \Sigma_{x_2} N_{12}(x_1, x_2)$, $n_2(x_2) = \Sigma_{x_1} N_{12}(x_1, x_2)$, and $n = \Sigma_{x_1}\Sigma_{x_2} N_{12}(x_1, x_2)$. The correlation ratio R is defined as*

$$R(x_1, x_2) = \sigma_{\text{tot}} \frac{\sigma_{12}^{\text{inv}}(x_1, x_2)}{\sigma_1^{\text{inv}}(x_1)\sigma_2^{\text{inv}}(x_2)}$$

$$= \sigma_{\text{tot}} \frac{N_{12}(x_1, x_2)/(\int L\,\mathrm{d}t)_{12}}{[N_1(x_1)/(\int L\,\mathrm{d}t)_1][N_2(x_2)/(\int L\,\mathrm{d}t)_2]}. \tag{2}$$

Here $\sigma_i^{\text{inv}}(x_i)$ is the invariant single-particle inclusive differential cross section for producing a particle with relative momentum x_i, $\int L\,\mathrm{d}t$ the appropriate integrated luminosity, and $N_i(x_i)$ the number of collected events per unit x_i in arm i. The quantities R and Q differ in an important manner, namely R contains both double- and single-arm data, while Q contains double-arm data only, making normalization unnecessary. In the absence of correlations, i.e. if $N_{12}(x_1, x_2)$ factorizes into a product $f_1(x_1)\cdot f_2(x_2)$, eq. (1) results in $Q = 1$, while eq. (2) factorizes into a product *which need not be equal to one*. If $\sigma_1^{\text{inv}}(x_1)$ and $\sigma_2^{\text{inv}}(x_2)$ do *not* contain any channels not present** in $\sigma_{12}(x_1, x_2)$, then $R = \text{const}\cdot Q$. On the other hand, if the single-particle cross sections do contain additional channels, then there is no simple relation between R and Q.

The expression for R in terms of normalized rates in (2) is exact only in the case of a point-like interaction region when the double-arm acceptance is equal to the product of the single-arm acceptances. The effects of a finite-size interaction region were checked by comparing R for subsets of events originating in different parts of the interaction diamond; this resulted in variations of less than 2%. Other systematic effects, resulting from efficiencies varying with time, from variations in the beam positions, and from differences in alignment between the two arms, were estimated (using high statistics $\pi\pi$ samples) to be below the level of 1%. Within the range $0.2 < p_T < 0.7$ GeV of the experiment the value of R was independent of p_T. An overall systematic check was made by determining $\sigma^{\text{inv}}(\text{pp} \to \pi^{\pm}\text{X}, \text{K}^{\pm}\text{X})$ from single-arm data. Good agreement was found with the results of ref. [1], both in absolute normalization and in x and p_T dependence. A detailed description of the data, the particle identification, and the analysis procedures can be found in ref. [3].

* Note that, as in ref. [6], we define the traditional correlation ratio R using σ_{tot}, and not σ_{inel}.

** For example, the channel $\text{pp} \to \text{p}\pi^+\text{n}$ will contribute to $\sigma_{\pi^+}(x_{\pi^+})$ but not to $\sigma_{\pi^+\pi^-}(x_{\pi^+}, x_{\pi^-})$.

2. Correlations for $\pi\pi$ pairs

Fig. 3 shows the correlation quotient Q for $\pi^+\pi^+$, $\pi^-\pi^+$, and $\pi^-\pi^-$ pairs as a function of x of one of the pions for specified intervals of the x of the pion in the other hemisphere, at $\sqrt{s} = 44.7$ and 62.3 GeV. It should be noted that the data run out well before the maximum value $x_1 = 1 - M^2_{\min}/\langle s(1-x_2)\rangle$ allowed by kinematics is reached. Here, $M^2_{\min}$ is the minimum missing mass recoiling against the $\pi\pi$ system: $(2M_n)^0$ for $\pi^+\pi^+$, $(2M_n)^{++}$ for $\pi^+\pi^-$, and $(2M_n + 2M_\pi)^{++++}$ for $\pi^-\pi^-$ combinations (M_n = nucleon mass). Fig. 4 shows the correlation ratio R for the same data (the data at $\sqrt{s} = 62.3$ GeV were also shown in ref. [2]). Table 1 gives the average values of Q (R) and χ^2/DF for the hypothesis $Q = \text{const.}$ ($R = \text{const.}$). It is apparent that Q is very close to one over the entire range in x_1, x_2, whereas R seems to vary slowly with x_1, x_2. Indeed, R is nearly constant, indicating that the single-particle inclusive cross section does not contain important channels that are not open to the two-particle cross section. As has been mentioned above, the result $Q = 1$ implies that R factorizes. We have therefore fitted the measured value of R with the product of two power expansions:

$$R(x_1, x_2) = \left(a_1 + b_1 x_1 + c_1 x_1^2\right)\left(a_2 + b_2 x_2 + c_2 x_2^2\right). \tag{3}$$

The fits (for $\sqrt{s} = 44.7$ GeV) are shown as solid lines in fig. 4. It is seen that this factorizing function of x_1 and x_2 fits the data reasonably well.

In order to investigate possible charge effects, we cast the data into the form of the ratio of π^+ to π^- yields in one spectrometer arm, for a π^+ or a π^- trigger in the other arm, and compare them with the inclusive π^+/π^- ratio. Fig. 5 shows the ratios

$$S^{\pm} = \frac{N(\pi^+ \text{ in Arm 1}, \pi^{\pm} \text{ in Arm 2})}{N(\pi^- \text{ in Arm 1}, \pi^{\pm} \text{ in Arm 2})},$$

versus x of the ratio π^+/π^- in Arm 1 for various values of x of the "trigger" pion in Arm 2. Also shown is the inclusive π^+/π^- ratio. It appears that, relative to the inclusive ratios, there are less π^+'s in Arm 1 when Arm 2 is triggered by a π^+ and that there are less π^-'s in Arm 1 when Arm 2 is triggered by a π^-. This trend is apparent only if the momenta of the π^+/π^- ratio are above $x \approx 0.5$ and seems to indicate a slight preference for the back-to-back $\pi\pi$ system to be electrically neutral.

The data discussed above support the hypothesis that there are no momentum correlations between the two back-to-back pions. It has been pointed out by Brodsky and Gunion [4] that the measurement of long-range correlations offers the possibility, within the context of counting rules, of distinguishing between gluon and quark exchange in the interaction. We refer to ref. [2]* for an extensive discussion of

* In ref. [2] it was stated, incorrectly, that an absence of correlations implies $R = 1$. As the measured ratios were close to one, the conclusions were not affected by this (overly restrictive) condition.

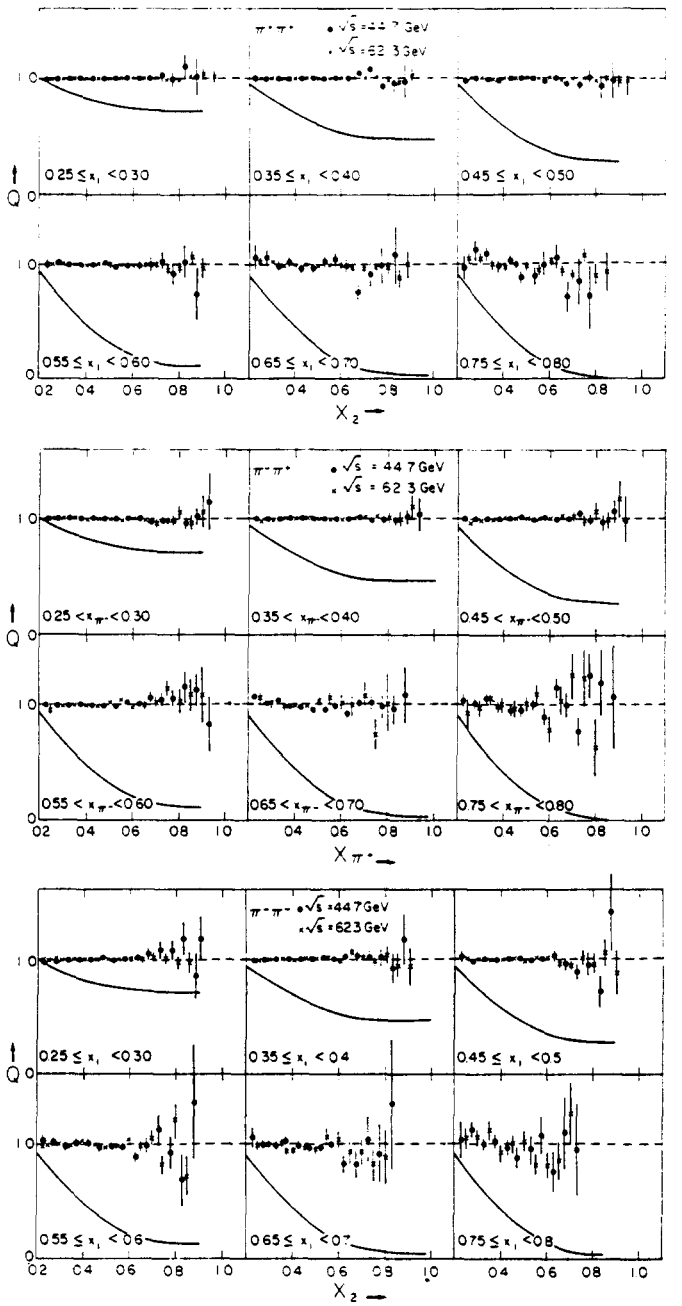

Fig. 3. The correlation quotient Q for the $\pi^+\pi^+$, $\pi^+\pi^-$, and $\pi^-\pi^-$ combinations as a function of the Feynman x of one of the pions for specified intervals of the x of the other pion at $\sqrt{s} = 44.7$ and 62.3 GeV. The predictions [2–4] for gluon exchange (dashed lines) and quark exchange in terms of the Brodsky-Gunion counting rules (solid lines) are shown also.

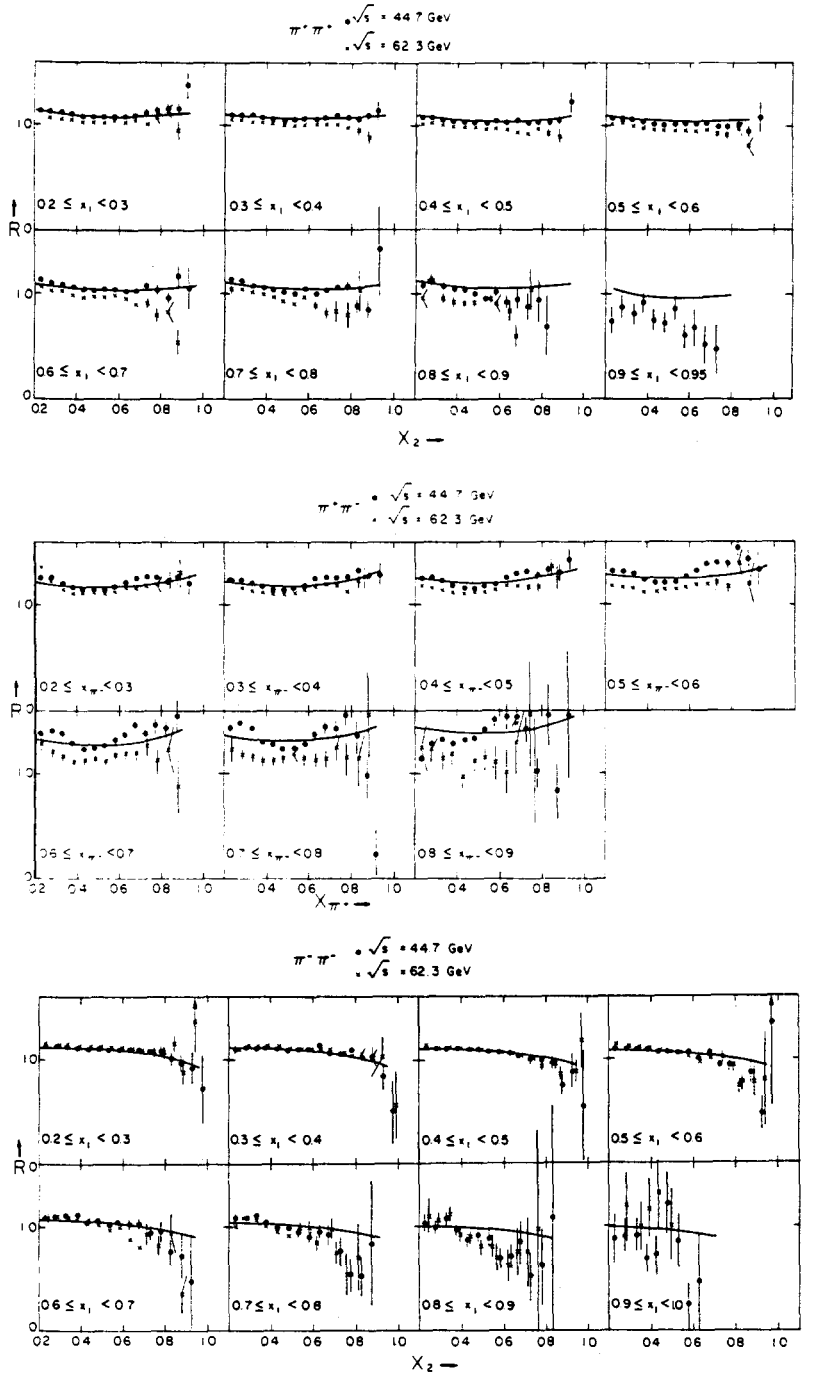

Fig. 4. The correlation ratio R for the $\pi^+\pi^+$, $\pi^+\pi^-$, and $\pi^-\pi^-$ combinations at $\sqrt{s} = 44.7$ and 62.3 GeV. The solid lines represent a fit to the data at $\sqrt{s} = 44.7$ GeV of a factorizing function of x_1 and x_2 as described in the text.

TABLE 1
Average values of Q and R for correlations involving π's and K's

Pair	$\sqrt{s}$ (GeV)	$\langle Q \rangle$	χ^2/DF	$\langle R \rangle$	χ^2/DF
$\pi^+\pi^+$	44.7	1.000 ± 0.001	1.10	1.091 ± 0.002	11
$\pi^+\pi^-$	44.7	1.000 ± 0.002	0.94	1.221 ± 0.002	22
$\pi^-\pi^-$	44.7	0.996 ± 0.005	0.92	1.121 ± 0.002	2.1
$\pi^+\pi^+$	62.3	1.000 ± 0.002	1.04	0.992 ± 0.002	3.2
$\pi^+\pi^-$	62.3	1.000 ± 0.001	1.01	1.151 ± 0.002	1.7
$\pi^-\pi^-$	62.3	1.000 ± 0.002	0.86	0.96 ± 0.01	1.8
π^+K^-	44.7	0.98 ± 0.02	0.70	1.21 ± 0.03	1.23
π^+K^+	44.7	1.00 ± 0.01	0.43	1.17 ± 0.01	1.83
π^-K^+	44.7	1.00 ± 0.01	0.66	1.24 ± 0.01	1.28
π^-K^-	44.7	0.97 ± 0.03	0.46	1.15 ± 0.04	0.99
K^+K^+	44.7	0.96 ± 0.04	0.70	1.21 ± 0.04	1.01
K^+K^-	44.7	0.92 ± 0.08	0.44	1.57 ± 0.10	0.76
K^-K^-	44.7			1.9 ± 0.7	0.11

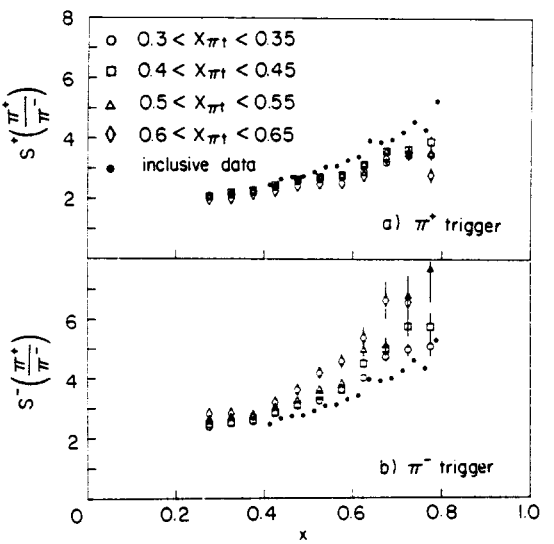

Fig. 5. (a) The π^+/π^- ratio S^+ in one spectrometer arm for specified intervals of the x of the π^+ trigger in the other arm; (b) the same for a π^- trigger. Comparison with the π^+/π^- ratio with no trigger in the other arm indicates an enhancement of neutral $\pi\pi$ pairs.

this point. The data presented here are an extension of those of ref. [2] and confirm the conclusion that gluon or sea-quark exchange together with the "valence-only" counting rule correctly describe both the momentum-dependence of inclusive single-particle spectra and the absence of two-particle momentum correlations.

3. Correlations for πK and KK pairs

Fig. 6 shows Q for the combination $\pi^+ K^+$. The data are consistent with $Q = 1$. Other combinations of charge of the πK pair behave in the same way. The average values of Q for the different combinations of charge are listed in table 1 and compared with the values found for the different charge combinations in $\pi\pi$ discussed above. Also given are the average values of R. They are all significantly different from one. Unlike the $\pi\pi$ data, the πK data are not accurate enough to distinguish between a constant and a factorizing x-dependence for R. Either conclusion would be in accord with factorization of the double differential cross section for the simultaneous production of a pion and a kaon.

Also given in table 1 are the average values of Q and R for the KK combinations. All $\langle Q \rangle$ values are compatible with one, indicating the absence of momentum correlations. The largest value of $\langle R \rangle$ occurs for the combination $K^+ K^-$, namely $\langle R \rangle = 1.57 \pm 0.10$, 4 standard deviations higher than the average for the other pairs.

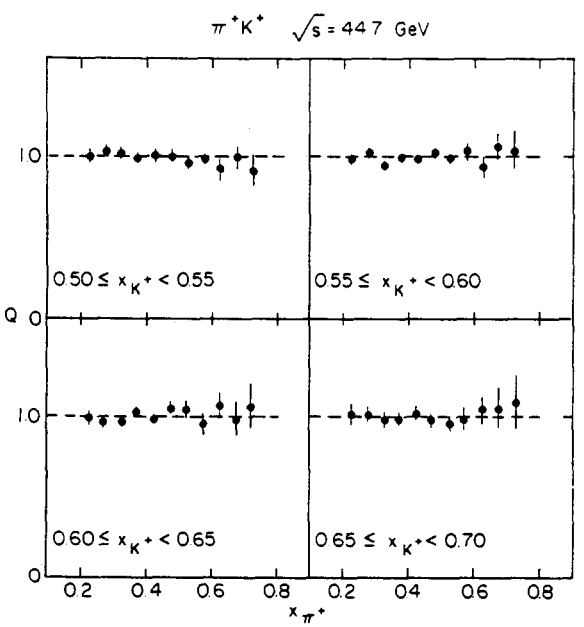

Fig. 6. The correlation quotient Q for $\pi^+ K^+$ pairs at $\sqrt{s} = 44.7$ GeV plotted versus x_{π^+}. The dashed line indicates the average value.

TABLE 2
Average values of Q for correlations involving protons at $\sqrt{s} = 44.7$ GeV

Pair	$\langle Q \rangle$	χ^2/DF	Range	$\langle R \rangle$	χ^2/DF
$p\pi^+$	0.988 ± 0.008	4.7			
$p\pi^+$	0.996 ± 0.005	1.05	$x_p < 0.95$	1.14 ± 0.01	2.7
$p\pi^-$	0.987 ± 0.008	2.5			
$p\pi^-$	0.995 ± 0.006	0.82	$x_p < 0.95$	1.25 ± 0.01	1.4
pK^+	0.94 ± 0.07	0.7			
pK^+	0.95 ± 0.06	0.6	$x_p < 0.95$	1.37 ± 0.05	1.1
pp	0.88 ± 0.03	37			
pp	0.955 ± 0.006	1.5	$x_p < 0.95$		
$p\Lambda$	0.991 ± 0.005	2.1			
$p\Lambda$	0.995 ± 0.004	1.1	$x_p < 0.95$		

This may be interpreted as a manifestation of "long-range" conservation of strangeness. A value of $\langle Q \rangle$ close to one ($\langle Q \rangle = 0.92 \pm 0.08$) is consistent with this interpretation. Evidence for "short-range" conservation of strangeness at high energy has been found in earlier work [5], where K^+ and K^- production in the same hemisphere, i.e. fragments from the same proton, have $\langle R \rangle_{K^+K^-} = 1.8 \pm 0.2$.

4. Correlations involving a final-state proton

In the process $pp \to pX$ the x dependence, at fixed p_T, of the final-state protons is determined by the combined effects of the elastic peak at $x_p = 1$, a broad diffractive peak in the range $0.95 < x_p < 1.0$ due to the coherent production of excited states of high mass, and a weakly x-dependent invariant cross section in the range $0.1 < x_p < 0.95$ as a result of inelastic scattering. One may therefore anticipate that small-angle particles produced in coincidence with a final-state small-angle proton in the opposite hemisphere will have $Q \neq 1$ if $x_p \gtrsim 0.9$, while for $x_p \lesssim 0.9$ the quotient Q is likely to be similar to that of $\pi\pi$ and πK pairs, i.e. $Q = 1$.

The data on correlations involving protons are summarized in table 2. The data on Q for $p\pi^+$, pp, and $p\Lambda$ are shown in figs. 7, 8a and 9a. The data on $p\pi^-$ and pK^+ (not shown) are similar in trend. In table 2 are listed the average values of Q and the χ^2 per degree of freedom for the hypothesis $Q = \text{const.}$, for all x_p and for the range $x_p < 0.95$. It is seen in table 2 that the fit is good only as long as diffractive protons are excluded, and that Q is close to one. Figs. 8b and 9b show the data on R_{pp} and $R_{p\Lambda}$ for $x_p < 0.95$*. A fit (dashed lines) to the hypothesis of a factorizing function in x_1 and x_2 [eq. (3)] has a satisfactory χ^2.

* The correlation rate R is strongly distorted towards low values if one of the particles is a proton with $x_p \gtrsim 0.95$. This is because the single-arm yields are dominated by elastic protons, while in the double-arm yield elastic protons are eliminated at the trigger level by the non-collinear positioning of the two spectrometer arms. The correlation quotient Q is not affected by this limitation.

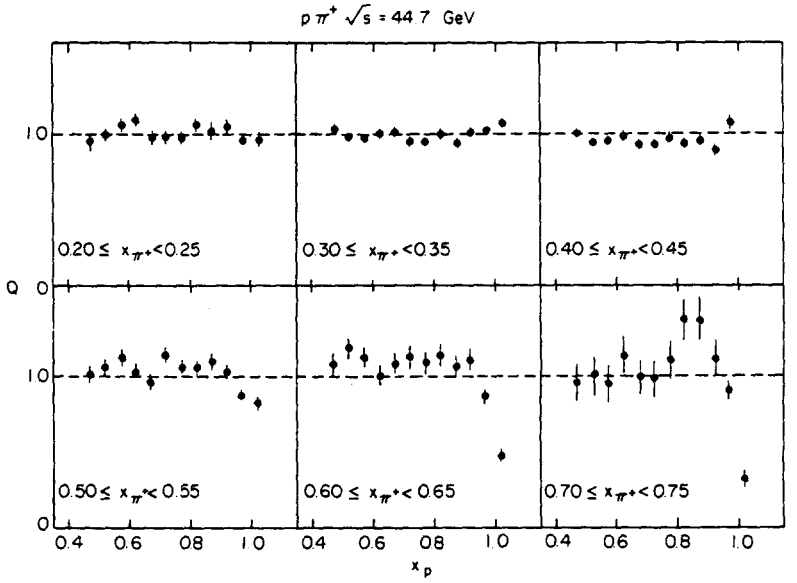

Fig. 7. The correlation quotient Q for $p\pi^+$ pairs at $\sqrt{s} = 44.7$ GeV plotted versus x_p.

A different way of looking at two-particle correlation data is in terms of the variable $z = (1 - x_1)(1 - x_2)$. In an approximation valid to better than 10^{-3} in the x and p_T range of this experiment, z is related to the missing mass recoiling against the two detected particles by $z = M^2/s$.

Fig. 10 shows the correlation ratio R as a function of z for $pp \to ppX$ and $pp \to p\Lambda X$. We observe that: (a) The data for $R(x_1, x_2)$ are not only consistent with a factorizing function of x_1 and x_2 but are also consistent with the hypothesis of scaling, i.e. a dependence on x_1 and x_2 through the single variable $z = (1 - x_1)(1 - x_2)$. An empirical parametrization of the mass dependence, in the form $R(z) = a + b\exp(-cz)$, is shown in fig. 8b and fits the data well. (b) The deviations from $R = \text{const.}$ in figs. 8b and 9b are associated with low missing masses, typically < 10 GeV. Put in words, we find that the probability for a ppX or $p\Lambda X$ final state exceeds the value expected from the product of the single-particle cross sections by an amount which depends on the missing mass M and increases as this mass becomes smaller.

Kwiecinski and Roberts [6] have pointed out that, assuming factorization, the presence of non-scaling terms in $pp \to pX$ gives rise to long-range correlations in $pp \to ppX$ of the form

$$R = 1 + c/\sqrt{zs}\,,$$

and depending on s as $\sim 1/\sqrt{s}$. This is shown in fig. 10a and is in good agreement

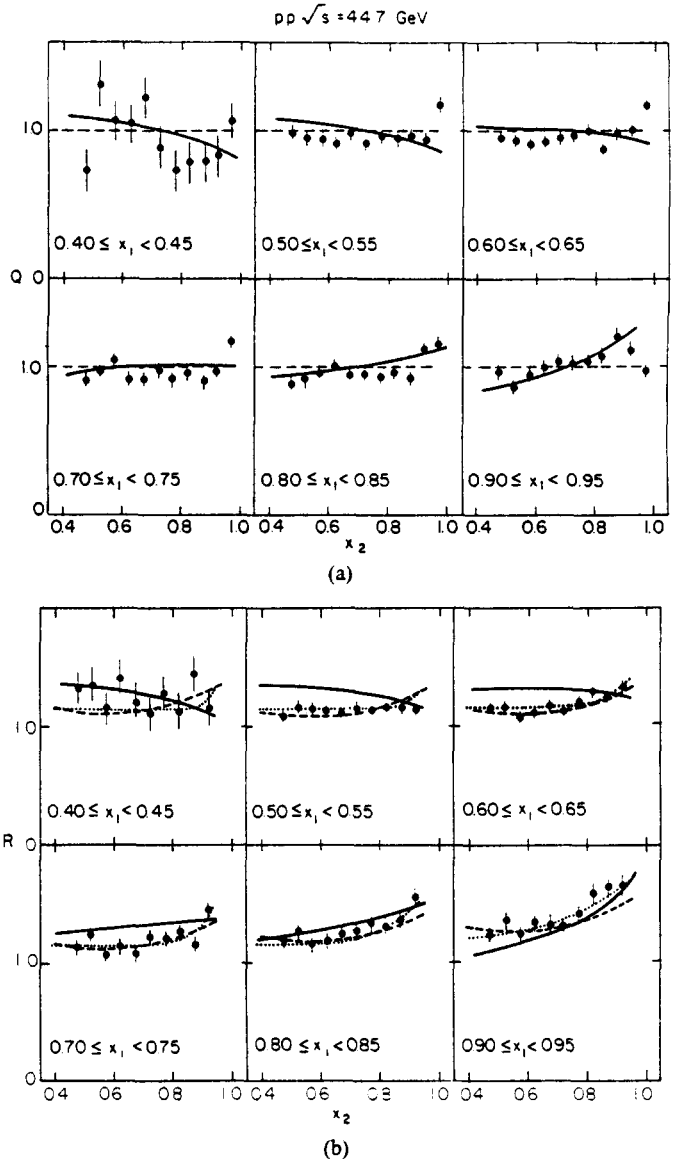

Fig. 8. (a) The correlation quotient Q, and (b) the correlation ratio R for pp pairs at $\sqrt{s} = 44.7$ GeV as a function of the Feynman x of one of the protons for specified intervals of the x of the other proton. The solid lines represent the model of Benecke et al. [8]. The dashed lines in (a) represent $Q = 1$, and in (b) the factorizing function of eq. (3). The dotted line in (b) represents a fit to the scaling function $R(z) = a + b\exp(-cz)$ as discussed in the text ($\chi^2/\mathrm{DF} = 0.96$, $a = 1.15 \pm 0.01$, $b = 0.67 \pm 0.07$, $c = 50 \pm 5$).

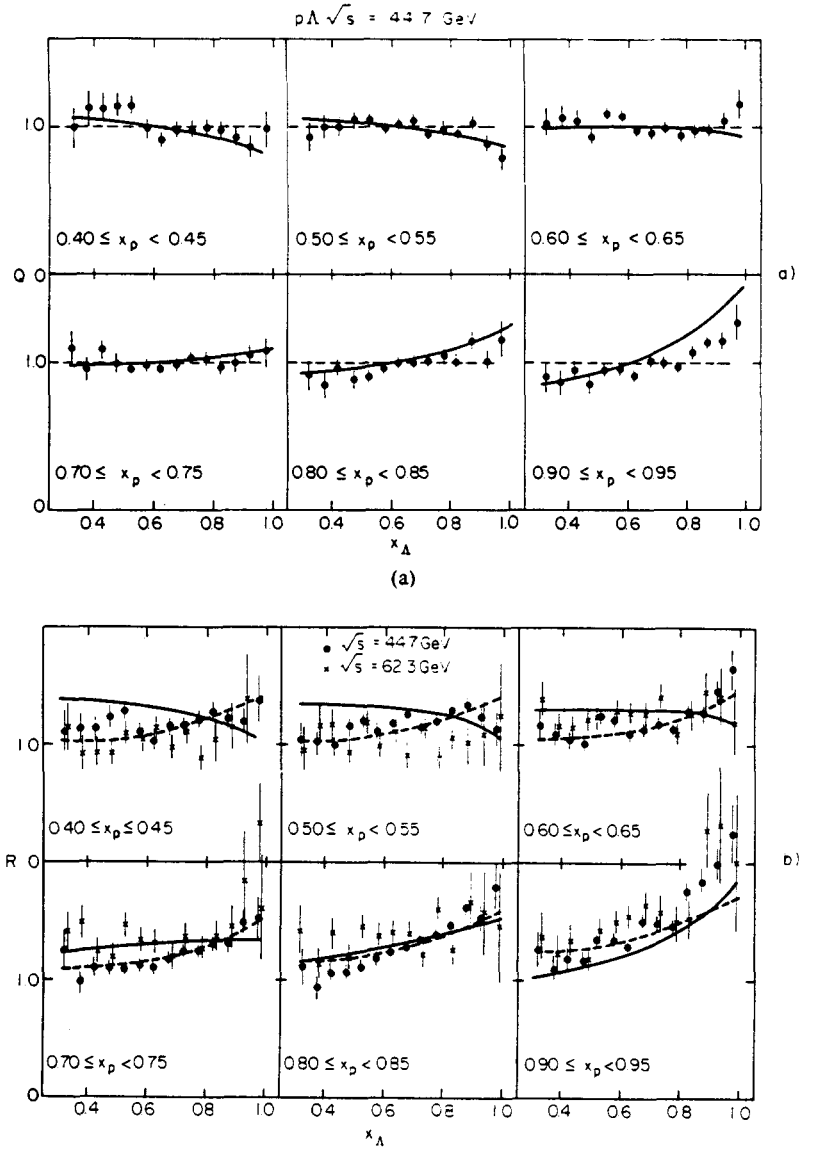

Fig. 9. (a) The correlation quotient Q at $\sqrt{s} = 44.7$ GeV, and (b) the correlation ratio R for pΛ pairs at $\sqrt{s} = 44.7$ and 62.3 GeV as a function of x_Λ for specified intervals of x_p. The solid lines represent the model of Benecke et al. [8]. The dashed lines in (a) represent $Q = 1$, in (b) the factorizing function of eq. (3).

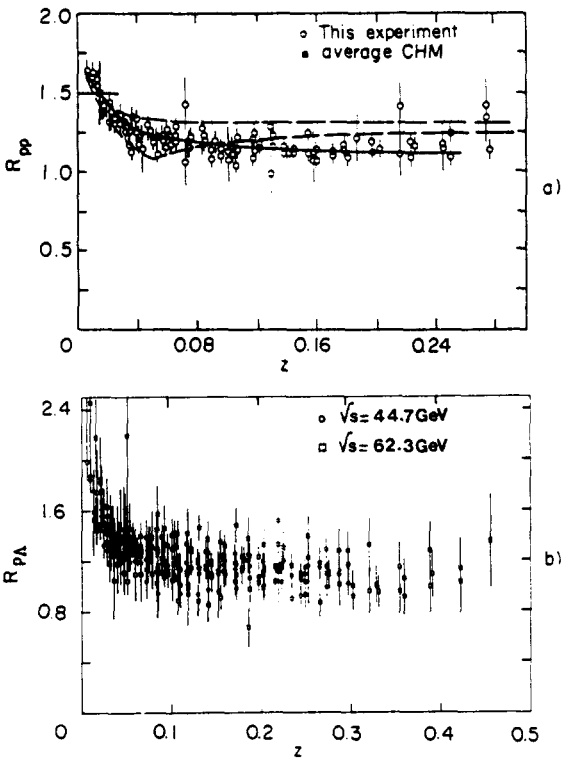

Fig. 10. The correlation ratio R (a) for pp and (b) for pΛ pairs, plotted as a function of the scaling variable $z = (1 - x_1)(1 - x_2)$. The solid line in (a) is a fit (χ^2/DF = 1.07, $c = 2.32 \pm 0.01$ GeV) to a model by Kwiecinski and Roberts [6]. The area enclosed by the dashed lines corresponds to a model by Benecke et al. [8]. The energy averaged point in (a) (CHM) is from ref. [7].

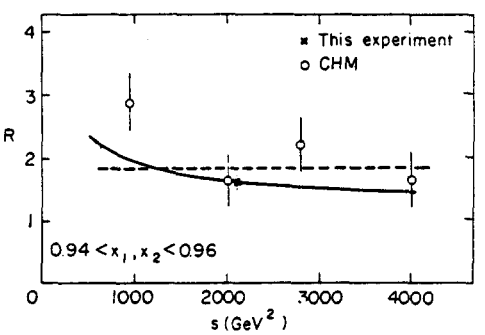

Fig. 11. The energy dependence of R(pp) at fixed x_1 and x_2 compared with the predictions of Kwiecinski and Roberts ([6], solid line) and of Benecke et al. ([8], dashed line). The CHM points are from ref. [7].

with the data. Fig. 11 shows the s-dependence of R_{pp}, based on the data of this experient and those of ref. [7]. There is no inconsistency, although the accuracy is limited.

Benecke et al., [8] and Miettinen [9] have proposed an independent emission model in which long-range correlations arise from correlated excitation of the colliding protons. In this model, R_{pp} and $R_{p\Lambda}$ can be calculated without free parameters* and are shown in figs. 8b and 9b. With plausible assumptions regarding the acceptance in x and p_T of the spectrometers, the x_1 and the x_2 dependence of Q_{pp} and $Q_{p\Lambda}$ have also been calculated and are shown in figs. 8a and 9a (solid lines). It may be concluded that the small deviations from $Q = 1$ and $R = \text{const.}$, notably the upward trend when both x_1 and x_2 are close to one, are in fact reproduced by this model. The correlations inherent in this model imply that R is not a factorizing function of x_1 and x_2. The dashed lines in fig. 10a indicate the values of R allowed by this model. The lack of factorization admitted by the finite accuracy of the data is seen to be consistent with the model. The s-dependence of the model is shown in fig. 11.

5. Summary

In the experiment described we have obtained the following results:

(i) In the inclusive production of two high-momentum mesons, each meson being emitted at small angles with respect to one proton beam, the correlation quotient Q has the value of one, and the correlation ratio R is a factorizing function of the two meson momenta. This result implies that the two fragmenting protons act independently.

(ii) The $\pi\pi$ data, although uncorrelated in momentum, seem to favour the formation of electrically neutral $\pi\pi$ systems.

(iii) The K^+K^- data exhibit strangeness conservation.

(iv) In $pp \to ppX$ and in $pp \to p\Lambda X$, the correlation ratio R is experimentally consistent with being either a factorizing or a scaling function of x_1 and x_2.

(v) The pp and $p\Lambda$ data have been compared with three mutually exclusive hypotheses: factorization, the Regge model of Roberts and Kwiecinski [6], and the independent emission model of Benecke et al. [8]. The data, within experimental accuracy, are consistent with each of the three models.

We would like to express our appreciation to the Physics Department of the University of Utrecht, where most of the equipment was constructed. We are grateful to the ISR Experimental Support, Vacuum, Operations, Power and Survey Groups for extensive assistance. We thank P. Kooyman and J. Timmer for contribu-

* For the calculation of $R_{p\Lambda}$ the x-distribution of the Λ was obtained from the proton x-distribution of ref. [8] by multiplication by $1 - x$.

tions to the early stages of the experiment. We have greatly appreciated the technical assistance of R. Bouhot. This work was supported by the Foundation for Fundamental Research on Matter, the Netherlands, the National Foundation for Scientific Research, Belgium, and a US Department of Energy grant.

References

[1] J. Singh et al., Nucl. Phys. B140 (1978) 189
[2] G.J. Bobbink et al., Phys. Rev. Lett. 44 (1980) 118
[3] G.J. Bobbink, Correlations between high momentum particles in proton-proton collisions at high energies, Ph.D. thesis, State University of Utrecht (1981)
[4] S.J. Brodsky and J.F. Gunion, Phys. Rev. D17 (1978) 848;
J.F. Gunion, Phys. Lett. 88B (1979) 150
[5] M.G. Albrow et al., Phys. Lett. 65B (1976) 295
[6] J. Kwiecinski and R.G. Roberts, Phys. Lett. 57B (1975) 349
[7] J. Timmer, Investigation of the reaction $p + p \rightarrow p + p + X$ at high energies, Ph.D. thesis, State University of Utrecht (1978)
[8] J. Benecke, A. Białas and S. Pokorski, Nucl. Phys. B110 (1976) 488
[9] H.I. Miettinen, Acta Phys. Pol. B6 (1975) 625